Nanoscale

PAPER

View Article Online
View Journal | View Issue

Cite this: *Nanoscale*, 2024, **16**, 9412

Novel PLGA-based nanoformulation decreases doxorubicin-induced cardiotoxicity†

Nikša Drinković,[a] Maja Beus,[b] Rinea Barbir,[b] Željko Debeljak,[c,d] Blanka Tariba Lovaković,[b] Nikolina Kalčec,[b] Marija Ćurlin,[e] Ana Bekavac,[f] Dunja Gorup,[g] Ivan Mamić,[h] Dario Mandić,[d] Vedran Micek,[b] Petra Turčić,[h] Nazende Günday-Türeli,[i] Emre Türeli[i] and Ivana Vinković Vrček *[b,j]

Nanotechnology has the potential to provide formulations of antitumor agents with increased selectivity towards cancer tissue thereby decreasing systemic toxicity. This *in vivo* study evaluated the potential of novel nanoformulation based on poly(lactic-*co*-glycolic acid) (PLGA) to reduce the cardiotoxic potential of doxorubicin (DOX). *In vivo* toxicity of PLGADOX was compared with clinically approved non-PEGylated, liposomal nanoformulation of DOX (LipoDOX) and conventional DOX form (ConvDOX). The study was performed using Wistar Han rats of both sexes that were treated intravenously for 28 days with 5 doses of tested substances at intervals of 5 days. Histopathological analyses of heart tissues showed the presence of myofiber necrosis, degeneration processes, myocytolysis, and hemorrhage after treatment with ConvDOX, whereas only myofiber degeneration and hemorrhage were present after the treatment with nanoformulations. All DOX formulations caused an increase in the troponin T with the greatest increase caused by convDOX. qPCR analyses revealed an increase in the expression of inflammatory markers IL-6 and IL-8 after ConvDOX and an increase in IL-8 expression after lipoDOX treatments. The mass spectra imaging (MSI) of heart tissue indicates numerous metabolic and lipidomic changes caused by ConvDOX, while less severe cardiac damages were found after treatment with nanoformulations. In the case of LipoDOX, autophagy and apoptosis were still detectable, whereas PLGADOX induced only detectable mitochondrial toxicity. Cardiotoxic effects were frequently sex-related with the greater risk of cardiotoxicity observed mostly in male rats.

Received 8th December 2023,
Accepted 16th April 2024

DOI: 10.1039/d3nr06269d

rsc.li/nanoscale

Introduction

Doxorubicin (DOX) is an anthracycline, a typical anticancer drug first isolated from *Streptomyces peucetius* in the 1960s.[1] It is still one of the most often prescribed effective antineoplastic agents developed for the treatment of a variety of cancers, such as ovarian, breast, gastrointestinal, Wilms tumor, and hematologic malignant tumors such as Hodgkin's and non-Hodgkin's lymphoma and pediatric leukemia.[2,3] Two mechanisms for the anticancer effect of DOX have been confirmed.[4] One of these relies on the interaction of DOX with the DNA resulting in the loss of DNA repair mediated with topoisomerase II.[5] The second one is related to oxidative stress of the cell membranes, DNA, and proteins with concomitant activation of NADH-dehydrogenase, NO synthase, xanthine oxidase, glutathione peroxidase, catalase, and superoxide dismutase, which can also initiate an inflammatory cascade.[6,7] Unfortunately, DOX's clinical application is associated with serious side effects like for many other cytotoxic substances,[8] including cardiomyopathy due to the formation of reactive oxygen species (ROS), apoptosis, inhibited expression of cardiomyocyte-specific genes, and altered molecular signaling in heart tissue.[9,10] Other side effects, such as gastrointestinal disturbances, vomiting, stomatitis, hallucinations, vertigo, and dizziness, are of an acute nature and primarily affect the patient's quality of life,[11] while cumulative and dose-related cardiotoxicity is one with the highest clinical significance as it may lead to congestive heart failure or even death.[12,13] DOX causes

[a]*Polyclinic Drinković, Zagreb, Croatia*
[b]*Institute for Medical Research and Occupational Health, Zagreb, Croatia. E-mail: ivinkovic@imi.hr*
[c]*JJ Strossmayer University of Osijek, Faculty of Medicine, Osijek, Croatia*
[d]*University Hospital Osijek, Osijek, Croatia*
[e]*Croatian Catholic University, Zagreb, Croatia*
[f]*University of Zagreb, School of Medicine, Zagreb, Croatia*
[g]*Department of Neuroradiology, Klinik für Neuroradiology, Universitätspital Zürich Universitätsspital Zürich, 8006 Zürich, Switzerland*
[h]*University of Zagreb, Faculty of Pharmacy and Biochemistry, Zagreb, Croatia*
[i]*MyBiotech GmbH, Überherrn, Germany*
[j]*University of Rijeka, Faculty of Medicine, Rijeka, Croatia*
† Electronic supplementary information (ESI) available. See DOI: https://doi.org/10.1039/d3nr06269d

dose-dependent cardiotoxic effects resulting in changes in myocardial structure that can further evolve to irreversible changes. The incidence of congestive heart failure ranges from approximately 3% up to 18% at the highest dose prescribed.[14] This cardiotoxicity represents one of the limiting factors towards DOX use in antitumor therapy.[15] Even more, the cardiotoxic effect caused by DOX increases with each dose due to irreversible myocardial damage.[16,17]

In order to minimize DOX-associated cardiotoxicity, various approaches have been utilized such as prolonged infusion for six hours or combining DOX with cardioprotective agents.[18,19] Unfortunately, meta-analyses of these approaches didn't show any differences in the clinical outcomes compared to applying DOX alone.[18,20] However, encapsulation of DOX into liposomal formulations proved to decrease its cardiotoxicity.[21,22] In general, liposomes can be designed to improve drug penetration, controlled release, and drug targeting thereby increasing drug efficacy while reducing toxic side effects.[23] Liposomal DOX formulations may favor the accumulation of the drug at tumor sites due to easier extravasation at sites of leaky vasculature (*i.e.* tumor sites) and, at the same time, reducing the ability to exit the circulation in healthy tissues, such as the heart, with its 'tight' endothelial capillary junctions.[24] Development of nano-enabled DOX formulations seems also promising. Two different nanoformulations for DOX have been approved for clinical use: non-PEGylated nanoliposomal DOX (Myocet™) and PEGylated nanoliposomal DOX (Caelyx®, Doxil®).[25] Clinical studies showed a reduction in cardiotoxic events for both of these cases, non-PEGylated[26–28] and PEGylated liposomal DOX.[29,30]

PEGylation is a process used to increase the stability of nanoliposomes by covalently linking polyethylene glycol (PEG) chains.[31] PEGylation increases the hydrophilicity of the nanoliposomes protecting them from phagocytic degradation and reducing their adhesion to various surfaces which in turn extends the half-life of the drug.[32] Another often-used polymer in the design of nanoformulations is poly(lactic-*co*-glycolic acid) (PLGA), a biodegradable and biocompatible material approved by both the U.S. Food and Drug Administration (FDA) and European Medicines Agency (EMA).[33] Scientific literature already evidenced in different animal models that PLGA-based nanoformulation reduce DOX cardiotoxicity.[34–36]

This study aimed to evaluate sex-related response and safety benefits of novel PLGA-based DOX nanoformulation (PLGADOX) produced by nanoprecipitation using the continuous MicroJet reactor technology.[37] Cardiotoxicity of this formulation was compared with clinically approved and used conventional DOX injection solution (ConvDOX) and non-PEGylated nanoliposomal DOX (LipoDOX). The study conducted repeated intraperitoneal administration of these 3 DOX formulations to healthy rats for 28 days (single administration every 5 days). Despite a number of studies published so far on PLGA-based DOX formulations, main novelty of our work is based on the experimental design to reveal sex-related cardiotoxicity of clinically used and new DOX formulations. Cardiotoxic effects were investigated by means of cardiac muscle damage, expression of inflammation-related genes, and impact on the metabolomic and lipidomic cardiac muscle profile.

Materials and methods

Drug formulations

DOX formulations used in this study were conventional doxorubicin injection solution (ConvDOX; Pliva, Zagreb, Croatia), commercial and clinically approved nanoliposomal formulation Myocet (LipoDOX; Teva, Petah Tikva, Israel) consisting of stable pluri-lamellar liposomes composed of egg phosphatidylcholine (EPC) and cholesterol with an aqueous core, and doxorubicin embedded in PLGA nanoparticles (PLGADOX) developed at MyBiotech GmbH (Überherrn, Germany). Characterization of lipoDOX and PLGADOX formulations was done as described previously by means of their shape, size, and size distribution, as well as surface charge after dilution with saline solution (see ESI†).[38]

Animal experiments

All animal experiments were approved by the Ethical Committee of the Croatian Ministry of Agriculture, Directorate of Veterinary and Food Safety, Department of Animal Welfare (Ethical Committee review number EP 320/2021; Animal Welfare approval class UP/I-322-01/21-01/08, urbr: 525-10/0543-21-4). Animal care was carried out in accordance with the EU Directive 2010/63/EU for animal experiments, with the Animal Protection Act (OG 135/06, 37/13) and with the Ordinance on the protection of animals used for experimental and other scientific purposes (OG 55/13). According to the recommendations of the European Society of Gender Health and Medicine, both sexes were included in the study: gender-specific differences were expected.

Wistar rats of both sexes, aged 12 weeks and weighing 320–350 g body weight (b.w.) for males (M) and 190–220 g b.w. for females (F), were bred under specific pathogen-free conditions at the Animal Breeding Unit, Institute for Medical Research and Occupational Health (IMROH), Zagreb, Croatia. Animals were acclimated in the controlled environment (temperature: 23 ± 2 °C; humidity: 55 ± 7% and light: 12 h light/dark cycle) and fed with standard GLP-certified food (Mucedola, 4RF21, Italy) and water *ad libitum*.

In total, 64 (32 F and 32 M) Wistar HsdBrlHan rats were used. Animals were randomly divided into 8 groups (4 male groups and 4 female groups, n = 8 per group): (1) control males treated with saline; (2) control females treated with saline; (3) males treated with ConvDOX; (4) females treated with ConvDOX; (5) males treated with LipoDOX; (6) females treated with LipoDOX; (7) males treated with PLGADOX; (8) females treated with PLGADOX. All treatments were done by intraperitoneal injections. The doses of applied formulations corresponded to 3 mg of the pharmacologically active substance (DOX) per kg of body weight (b.w.). Doses were determined by consulting the relevant scientific literature.[39–42] All formulations were diluted in saline. All animals received 5

doses of tested substances at intervals of 5 days, administered on days 1, 6, 11, 16, and 21. On the fifth day after the last administration, animals were sacrificed under general anesthesia using an anesthetic cocktail (Narketan, Vetoquinol UK Ltd, 80 mg per kg b.w.; Xylapan, Vetoquinol UK Ltd, 12 mg per kg b.w., i.p.) in order to avert any pain caused by exsanguinations and tissue harvesting. All gross pathological changes of the internal organs were examined by a licensed veterinarian. The blood samples were collected in heparinized vacutainers (Becton, Dickinson and Co., Rutherford, New Jersey, USA) by dissection of the carotid artery under general anesthesia. Blood was centrifuged (1200*g*, 10 min, at 4 °C), obtained serum was frozen at −80 °C and further used for markers of cardiac toxicity, namely troponin T (TnT) and rat N-terminal prohormone of brain natriuretic peptide (NT-proBNP). After washing in ice-cold physiological saline, hearts were divided into small pieces and stored in formalin for the pathohistological diagnosis (PHD), in RNA Later (Thermo Fisher Scientific Inc., Schwerte, Germany) for mRNA expression analysis using quantitative polymerase chain reaction (qPCR), or in the cryopreservation tubes at −80 °C for matrix-assisted laser desorption/ionization (MALDI) mass spectrometry imaging (MSI) analysis.

Pathohistological evaluation of heart tissues

Pieces of heart tissues were put in 50 mL Falcon tubes (Eppendorf, Hamburg, Germany) containing 4% (v/v) formaldehyde (BioGnost, Zagreb, Croatia) immediately after removing the organs from the animals and were left in fixative for 7–10 days. Afterward, the organs were transferred to cassettes and rinsed overnight with distilled water. The next day, heart tissues were dehydrated by a series of ethanol dilutions (from 50% to 100% (v/v)). The organs were then embedded in paraffin. The details on dehydration and paraffin embedding are given in Tables S1 and S2 (ESI†). Tissue sections of 8 μm were cut on a rotary microtome and the prepared slides were stained with hematoxylin and eosin (H&E; Biognost, Zagreb, Croatia) as described in Table S3 (ESI†). Two histological slides were prepared, each slide containing two sections, to ensure backup in the case of poorly made sections causing the morphology of the organ to not be ideally preserved. After staining, histological slides were analyzed using an Olympus fluorescence microscope Olympus BX53F2 (Olympus, Tokyo, Japan).

Determination of cardiac biomarkers

Determination of TnT and NT-proBNP in serum samples was performed using the enzyme-linked immunosorbent assay (ELISA) kits purchased from MyBioSource Inc. (San Diego, USA). Measurements were performed according to the manufacturer's instructions. The color change was measured spectrophotometrically at a wavelength of 450 nm ± 10 nm on a Victor3™ plate reader. The concentrations of TnT and NT-proBNP in the samples were determined by comparing the optical density (O.D.) of the samples to the standard curves.

Evaluation of oxidative stress response

Intracellular ROS in heart tissue homogenates were measured using 2′,7′-dichlorofluorescin diacetate (DCFH-DA) and dihydroethidium (DHE) staining assays. In the presence of a superoxide radical, DHE is oxidized to a fluorescent 2-hydroethidium allowing the accurate measurement of fluorescence signals which correlate with the amount of superoxide radical. The DCFH-DA is converted by cellular esterase into non-fluorescent 2′,7′-dichlorofluorescin (DCFH), which is then oxidized to the fluorescent DCF product in the presence of hydroxyl radical. The procedures were performed as previously described.[43] An ice-cold 40 mM Tris-HCl buffer (pH 7.4) was used for diluting fresh 10% (w/v) tissue homogenates to 0.25% (w/v) homogenates which were pipetted into wells of 96-well plate following the addition of 20 μL 0.12 mM DCFH-DA or DHE. Autofluorescence was examined by preparing the tissue without the addition of a dye. After incubating the samples for 20 min at 37 °C fluorescence was determined at the 488 nm excitation and 525 nm emission wavelengths using a fluorescence plate reader Victor3™ (PerkinElmer, Shelton, USA).

A monochlorobimane (MBCl) fluorescent probe, highly specific for glutathione (GSH) detection, was used for measuring the GSH level in heart tissue. Diluted 0.25% (w/v) tissue homogenates were prepared in the 40 mM Tris-HCl buffer (pH 7.4) and placed on ice prior to analysis. Furthermore, 0.1 mL of 0.25% homogenate portions were pipetted into wells of a 96-well plate following the addition of 20 μL of 0.24 mM MBCl. Autofluorescence was examined by preparing the tissue without the addition of a fluorescent probe. All samples were incubated for 30 min at 37 °C. Fluorescence was determined at the 355 nm excitation and 460 nm emission wavelengths using a Victor3™ plate reader. Results are obtained as relative fluorescence units (RFU) and all results for the level of hydroxyl radicals, superoxide radicals, and GSH of heart tissue were normalized based on total protein content (RFU per mg protein). QuantiPro BCA assay kit (QPBCA, Merck KGaA, Darmstadt, Germany) was used for protein quantification according to the manufacturer's instructions. Final data are represented as mean values obtained from eight animals including standard deviations (SD). Significant differences ($p < 0.05$) between controls and treated animals are indicated by the asterisks (*).

mRNA expression analysis

Heart tissues were transferred from RNALater to tubes containing Aurum Lysis Solution (Bio-Rad, Hercules, California, USA) and were homogenized using the dispenser Ika Ultra-Turrax T10 (IKA Works, Inc.) for 30 s in the ice bath. RNA was isolated from tissue homogenates using Aurum total RNA mini kit (Bio-Rad, cat. 732-6820) according to the manufacturer's instructions. RNA was then transcribed to cDNA using the high-capacity DNase reverse transcription kit (Thermo Fisher Scientific Inc., Schwerte, Germany) according to manufacturer's instructions. 5 μL of isolated RNA sample was added per 10 μL of reverse transcription reaction, which proceeded in

Biosan TS-100C thermomixer (Biosan TS-100C thermomixer) using the manufacturer's program.

The qPCR analysis was performed using the iTaq Universal SYBR green Supermix kit (BioRad, California, USA) in the twin.tec 96-well plates (Eppendorf, Hamburg, Germany) on Applied 7500 PCR System (Applied Biosystems, Foster City, CA, USA). Reaction mixtures were prepared using 10 μM primer stock solutions (diluted to a final concentration of 200 nM) with a final reaction volume of 20 μL per sample. The negative control for reverse transcription reaction was no template RT control, whereas the absence of PCR-product/cDNA contamination was assessed by the inclusion of a no template control (NTC) in every run. In both cases, ultrapure sterile water was added instead of sample RNA or cDNA, respectively. Each sample was tested in triplicates for the expression of each gene. cDNA was added to tubes containing iTaq Universal SYBR Green Supermix and primers. Primers (Metabion, Planegg, Germany) were used for IL-6 (forward: ATATGTTCTCAGGGAGATCTTGGAA; reverse: GTGCATCATCGCTGTTCATACA), IL-8 (forward: CTCCAGCCACACTCCAACAGA, reverse: CACCCTAACACAAAACACGAT), TNF-alpha (forward: GGCTGCCCCGACTATGTG, reverse: CACCCTAACACAAAACACGAT), IL-1b (forward: CCAGGATGAGGACCCAAGCA, reverse: TCCCGACCATTGCTGTTTCC). GADPH (forward: TGGCACAGTCAAGGCTGAGA, reverse: GATCGCGCTCCTGGAAGAT) was used as a reference gene. The reaction was performed using the following program: 1 cycle for 30 s at 95 °C (polymerase activation), followed by 40 cycles of 15 seconds at 95 °C, then 60 seconds at 60 °C (PCR cycling). Relative quantities, *i.e.* relative mRNA levels of target genes were calculated using the $2^{-\Delta\Delta Cq}$ method, which calculates fold changes as recommended by Hellemans *et al.*[44] The normalization was performed against reference gene GADPH.

MSI analyses

Cryopresrevd heart tissue samples were cut into longitudinal sections 6 μm thick on a Leica CM1950 cryostat (Wetzlar, Germany), at the temperature of −20 °C. All samples were mounted on indium tin oxide (ITO) coated glass slides (Sigma Aldrich, St Louis, USA; sheet resistance of 15–25 Ω sq^{-1}) and analyzed immediately. Due to the complexity and reproducibility of the IMS, 2 randomly selected samples per group were analyzed.

All MSI experiments were performed using iMScope Trio (Shimadzu, Kyoto, Japan). The instrument was equipped with a light microscope, Nd:YAG LASER (355 nm), containing an atmospheric pressure MALDI source and an ion-trap (IT) TOF MS running in the reflectron mode. Optical images of the samples were taken first using the in-built microscope of the iMScope Trio (Shimadzu, Kyoto, Japan) in transmission mode, at 100× magnification. Then, the slides were overlaid with a 2,5-dihydroxybenzoic acid (DHB; Sigma Aldrich, Germany) matrix by sublimation procedure lasting 25 min using iMLayer (Shimadzu, Kyoto, Japan). Recrystallization was performed in a closed container heated to 70 °C for 105 s using 5% (v/v) methanol : water solution. ITO slides covered with the matrix were placed above the solution. Following matrix deposition, the optical images were recorded again, in transmission mode, at 25× magnification.

Examination of different instrument settings yielded the optimized parameters as follows. Samples were recorded in positive mode, with ranges of 200–650 *m*/*z* and 650–1000 *m*/*z*. 420 pixels (14 × 30) per sample were recorded, sample voltage of 3.5 kV and a detector voltage of 2.1 kV. Accumulation was 1 time/pixel, number of laser shots 100, frequency of 500 Hz, diameter 2, and intensity 50%. DHB was used for instrument calibration. Selected *m*/*z* ranges enabled the analysis of the content of spermine, ceramide (Cer), lysophosphatidylcholine (LysoPC), and acylcarnitine (Car).

Acquired MS images were generated and analyzed using IMAGEREVEAL v1.1 (Shimadzu, Kyoto, Japan). Before further analysis was performed all *m*/*z* values were normalized by total-ion-current method.

Statistical analysis

One-way ANOVA testing with *post hoc* Tukey test was performed for the statistical analysis of cardiac markers TnT and NT-proBNP, and parameters of the oxidative stress response, whereas one-way ANOVA with *post hoc* Dunnett's multiple comparison tests was performed for mRNA expression analysis. The treatment groups were compared with the control group ($p < 0.05$). Mean and SEM were plotted on column graphs. GraphPad Prism 6.0 software was used for statistical analysis and graphical representation. Results from MALDI-MSI experiments are represented as a heat map that was generated using log2ratio of average *m*/*z* intensities and the statistical program R ver. 4.2.0.[45]

Results and discussion

Physico-chemical characteristics of DOX nanoformulations

Nanoformulations LipoDOX and PLGADOX in saline solutions were characterized by using dynamic light scattering (DLS), electrophoretic light scattering (ELS), and transmission electron microscopy (TEM) techniques. Both nanoformulations had spheroidal shapes as can be seen in TEM micrographs (Fig. 1). LipoDOX had a smaller hydrodynamic diameter (d_H) of 126.2 ± 1.4 nm, whereas the d_H of PLGADOX was measured to be 252.4 ± 12.7 nm (Fig. 1). According to dynamic light scattering (DLS) measurements, both nanoformulations were uniform in size with a monomodal distribution, although TEM micrographs showed some aggregates, probably generated during sample preparation (drying) for TEM measurements. The ζ potential indicated a negative charge for both formulations, −48.3 ± 0.8 mV for LipoDOX and −12.9 ± 0.4 mV for PLGADOX formulations.

Stability evaluation of LipoDOX and PLGADOX in saline solution was also performed by DLS, ELS, and TEM measurements and showed good colloidal stability with no changes in shapes, d_H, and ζ potential values during 24 h. Thus, these results confirmed the quality attributes of both formulations.

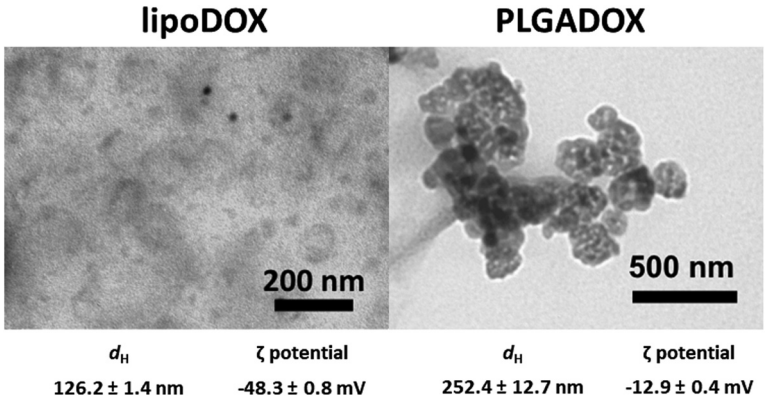

Fig. 1 Physico-chemical characteristics of LPS and PLG formulations. Transmission electron micrographs of non-PEGylated liposomal formulation of doxorubicin (LipoDOX; left, scale bar of 200 nm), and PLGA-liposomal formulation of doxorubicin (PLGADOX; right, scale bar of 500 nm). Hydrodynamic diameters (d_H, nm) were obtained by DLS, and ζ potential (mV) was measured using the ELS method. All measurements were done at 25 °C.

Pathohistological analysis of heart tissues

DOX is known to induce apoptosis in cardiomyocytes, thereby directly damaging the heart tissue.[46] Histopathological analysis of hearts of both female and male rats treated with ConvDOX showed signs of myofiber necrosis (Fig. 2a–e). Necrotic changes were characterized by loss of cellular and nuclear details and myofiber vacuolation (Fig. 2a). Additionally, degeneration processes were also observed in both sexes, indicated by the presence of preapoptotic eosinophilic cells (Fig. 2b). The latter was not surprising since DOX's mechanism of action involves the induction of apoptosis.[47] Similar observations were reported in an earlier study after 15-day treatment with 2 doses of DOX.[48] Some of the changes were sex-related, such as the waves of fibrils in males (Fig. 2c) and loss of preexisting fibers (myocytolysis) in females (Fig. 2d). Additionally, the signs of hemorrhage were found only in male rats (Fig. 2e), probably due to the higher concentration of estrogen in female rats, which is known to protect from hemorrhage.[49,50]

Results observed for DOX nanoformulations confirmed previous findings that the incorporation of drugs into nanocarriers can enhance their selectivity towards cancer tissue thereby minimizing unwanted toxic effects.[24] Indeed, less severe histopathological changes were found in the hearts of rats treated with LipoDOX or PLGADOX (Fig. 2f–k). Compared to ConvDOX, treatment of female rats with LipoDOX resulted in weaker signs of myofiber necrosis characterized by loss of cellular detail, myofiber vacuolation, and waves of fibrils (Fig. 2f and g) along with preapoptotic eosinophilic cells (Fig. 2f). In males, only the signs of hemorrhage were found (Fig. 2h). Only small histopathological changes were observed in the hearts of rats treated with PLGADOX. Hearts of female rats showed only weak signs of early stages of myofiber degeneration characterized by preapoptotic eosinophilic cells (Fig. 2i), whereas signs of necrosis (loss of cellular details associated with preapoptotic eosinophilic cells), cellular infiltration, and hemorrhage were found in the heart of male rats (Fig. 2j and k).

In general, all of the heart tissues showed signs of apoptosis, but this was less pronounced in animals treated with LipoDOX and PLGADOX compared to ConvDOX.

Effect of different DOX formulations on cardiac biomarkers

To assess DOX-related cardiac muscle damage, different biomarkers can be evaluated to provide insight into various biological processes.[51] Cardiac troponins I (cTnI) and T (cTnT) have been shown to be highly sensitive and specific markers of myocardial cell injury. Serum levels of TnT are of diagnostic value for myocardial damage in various conditions, including myocardial infarction.[52,53] NT-proBNP is a marker that is released from ventricles in response to pressure and volume overload. Raised plasma level of NT-proBNP is seen in ventricular dysfunction, ventricular muscular mass reduction, or ventricular ischemia.[53] Earlier studies have shown a correlation between the cardiotoxicity induced by DOX and other anthracyclines and increased levels of cardiac markers at the end of treatment.[54,55]

All DOX formulations significantly increased the concentration of TnT in male rats (Fig. 3a), indicating cardiotoxicity as early increases in TnT indicate the risk of cardiotoxicity following DOX therapy. A similar correlation between higher TnT concentrations and cumulative DOX doses was observed earlier.[56,57] In female rats, a significant TnT increase was seen only after treatment with ConvDOX and LipoDOX, while PLAGDOX treatment did not affect TnT plasma level in female rats (Fig. 3b).

This finding indicates reduced cardiotoxicity of PLGADOX, which was further confirmed by the measurement of NT-proBNP. This cardiac marker is elevated after acute heart failure, but its low level has been indicated as an early sign of ischemic heart failure.[58] Various research groups reported similar findings,[59,60] and measurement of NT-proBNP has been suggested after the end of chemotherapy treatment.[61] Interestingly, only LipoDOX significantly decreased its value in both male and female rats (Fig. 3c and d), while PLGADOX

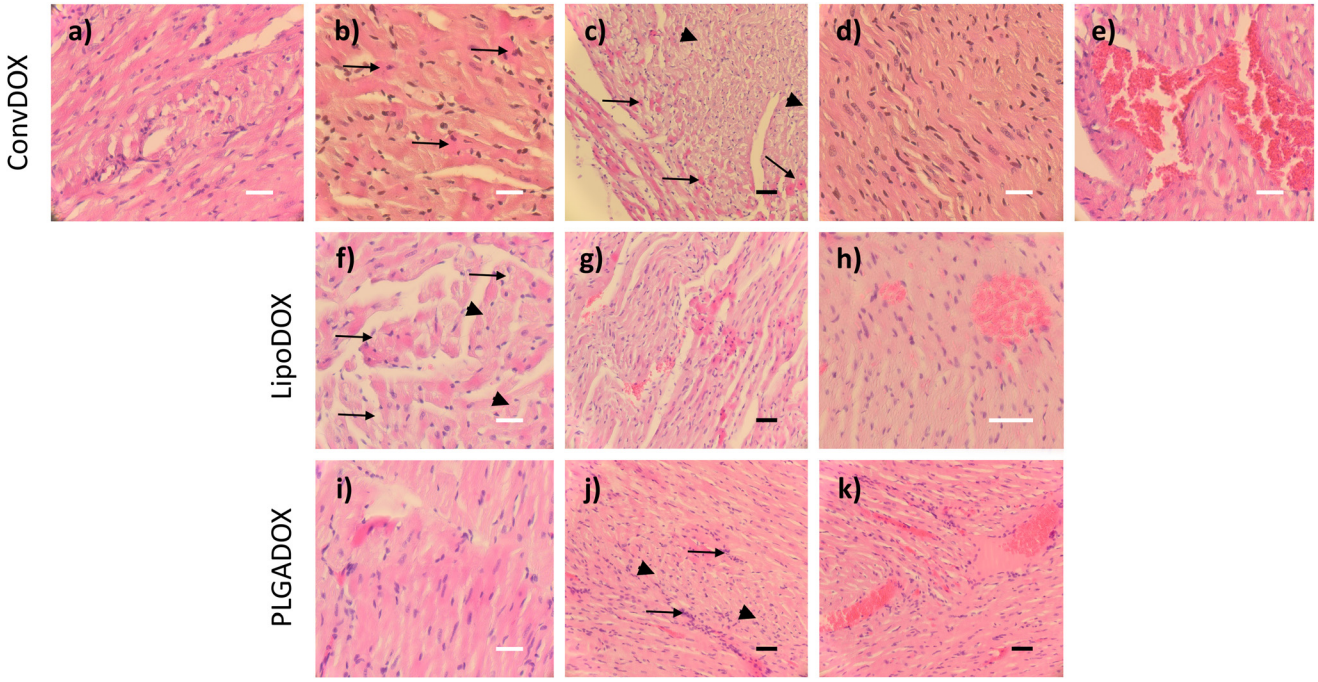

Fig. 2 Histopathological effects of conventional doxorubicin (ConvDOX; a–e), non-PEGylated liposomal formulation of doxorubicin (LipoDOX; f–h), and PLGA-liposomal formulation of doxorubicin (PLGADOX; i–k) in heart tissues of rats. (a) Male rats treated with ConvDOX show myofiber necrosis with loss of cellular detail and vacuolation; (b) arrows indicate preapoptotic eosinophilic cells ConvDOX-treated male rats; (c) arrow heads indicate loss of preexisting fibers (myocytolysis), and arrows indicate preapoptotic eosinophilic cells in ConvDOX-treated females; (d) waves of fibrils present in male rats treated with ConvDOX; (e) hemorrhage is present in the hearts of male rats treated with ConvDOX; (f) loss of cellular detail (arrowheads), myofiber vacuolation (arrows) and preapoptotic eosinophilic cells are present in the heart of female rat treated with LipoDOX; (g) waves of fibrils and preapoptotic eosinophilic cells present in the heart of female rat treated with lipoDOX; (h) hemorrhage is present in the hearts of male rats treated with LipoDOX; (i) heart of female rat treated with PLGADOX showing the presence of preapoptotic eosinophilic cells; (j) heart of male rat treated with PLGADOX showing loss of cellular detail (arrowheads), preapoptotic eosinophilic cells and cellular infiltration (arrows); (k) hemorrhage is present in the hearts of male rats treated with PLGADOX. Black bars indicate 50 μm (20× magnification), whereas white bars indicate 20 μm (40× magnification).

treatment did not affect NT-proBNP levels either in male or female rats. These findings are well supported by histopathological analysis, which showed the weakest damage in heart tissues of female rats treated with PLGADOX compared to the other two DOX formulations (Fig. 2).

Oxidative stress response in heart tissue following treatment with different DOX formulations

The mechanism of DOX-induced cardiotoxicity has not been fully elucidated, but many studies showed that different mechanisms are involved including oxidative damages, inflammation and apoptosis of cardiomyocytes leading to the progression of cardiomyopathy after cumulative doses.[62] Cardiotoxicity can occur even after a single dose of the drug or over a longer period of time (from several weeks to months).[63] The cytotoxic effect of anthracyclines on cardiomyocytes is generally considered to be irreversible and related to the cumulative dose.[64] Cardiac mitochondria are the preferred target of DOX and accumulate the drug in relatively high concentrations. Cardiac mitochondria are particularly prone to DOX-induced oxidative damage, and at the same time are important sources of DOX-induced ROS.[65] DOX can be a substrate of several oxidoreductases such as mitochondrial complex I NADH-dehydrogenase and various cytoplasmic oxidoreductases, including xanthine oxidase. The oxidoreductive reaction begins with the transfer of one electron from NADPH to DOX, thus forming a semiquinone radical that forms a complex with iron. This complex is responsible for the reduction of oxygen, thus creating the superoxide ion.[66] The formation of a complex between DOX and phospholipids leads to the inhibition of mitochondrial enzymes that participate in oxidative phosphorylation. Damage to the mitochondrial membrane can also lead to the inactivation of key transporters involved in ion homeostasis. Therefore, the cardiotoxicity of anthracyclines could be simply explained by the fact that heart tissue is rich in mitochondria. However, other factors are also involved in the cardiotoxicity of anthracyclines, among which is a relatively smaller amount of antioxidant defense of the heart compared to other tissues.[66] Because of this, free radicals accumulate in heart tissue and cause lipid peroxidation and destruction of cell and mitochondrial membranes, endoplasmic reticulum, nucleic acids and intracellular macromolecules.[63]

Levels of peroxy and superoxide radicals in the heart tissue of control and treated male and female Wistar rats were determined by DCFH-DA and DHE assays, respectively. As in the

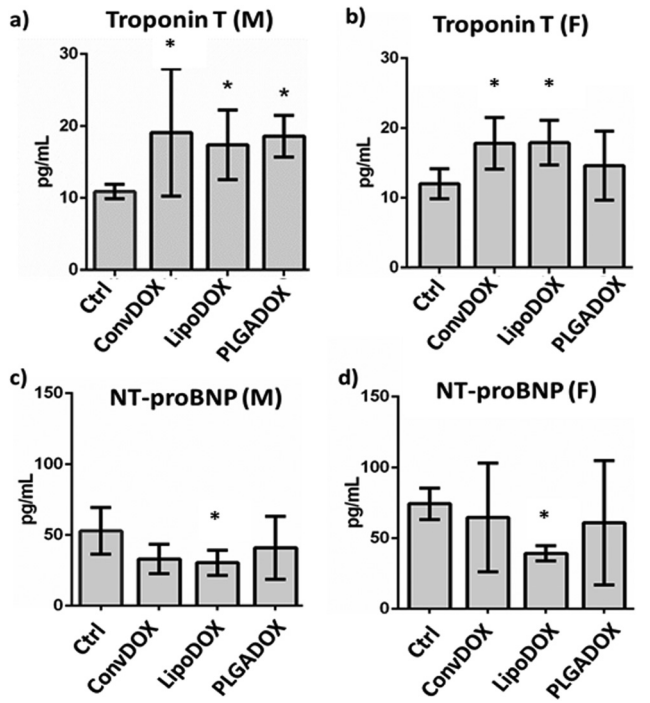

Fig. 3 Effect of different doxorubicin formulations on the concentration of biomarkers used for cardiotoxicity evaluation. (a and b) Concentration of troponin T, and (c and d) N-terminal natriuretic peptide (NT-proBNP) determined in animal serum of male (M) and female (F) rats treated with conventional doxorubicin (ConvDOX), non-PEGylated liposomal formulation of doxorubicin (LipoDOX), and PLGA-based nanoformulation of doxorubicin (PLGADOX). Results are presented as average values ± standard error of the mean values (SEM). Significant differences ($p < 0.05$) between treated and control animals are denoted with an asterisk (*).

case of serum cardiac injury markers (Fig. 3), a different response was observed between males and females. In males, a significant increase in superoxide radical level was observed for ConvDOX treatment, while PLGADOX treatment resulted in a significantly reduced level of these radicals compared to Ctrl (Fig. 4a). In females, no significant differences between control and treated animal groups were found for superoxide radicals level (Fig. 4a), but ConvDOX treatment significantly increased, while PLGADOX significantly decreased peroxy radicals in heart tissue compared to control animals (Fig. 4b). When comparing these results with the measured levels of GSH, weaker pathohistological changes in females compared to males treated with PLGADOX can be explained by the protective action of antioxidant GSH and its main role in reducing reactive oxygen species (ROS). Indeed, PLGADOX-treated females had significantly increased GSH level compared to control females (Fig. 3c), which indicate the induction of antioxidant cellular mechanisms. Although the protective effect of GSH against DOX-induced toxicity has been demonstrated,[67,68] molecular mechanisms related to its protective actions are unknown. Decreased levels may result from increased oxidation or increased conjugation to proteins and drugs.[69] Thus, increased GSH reduced the level of peroxy radical in heart tissue of PLGADOX-treated female rats. Similar results were observed for LipoDOX-treated females, while this was not observed for males (Fig. 4b and c). These results corroborate quite well with results obtained by histopathological analysis and serum cardiac markers TnT and NT-proBNP.

Inflammatory response in heart tissue

DOX is known to cause inflammation in various organs leading to poor prognosis.[70–72] It has been demonstrated already that DOX treatment leads to an inflammatory response in the myocardium triggering the release and induction of proinflammatory and chemoattractant cytokines (TNFα, IL-6, IL-8, IL-1β) by cardiomyocytes and cardiac fibroblasts and inducing the expression.[16,73,74] The mRNA expression profile in heart tissue of male and female rats following treatment with different DOX formulations as compared with non-treated animals are presented in Fig. 5. Expression of all tested cytokines, except IL-1β, was significantly increased in males

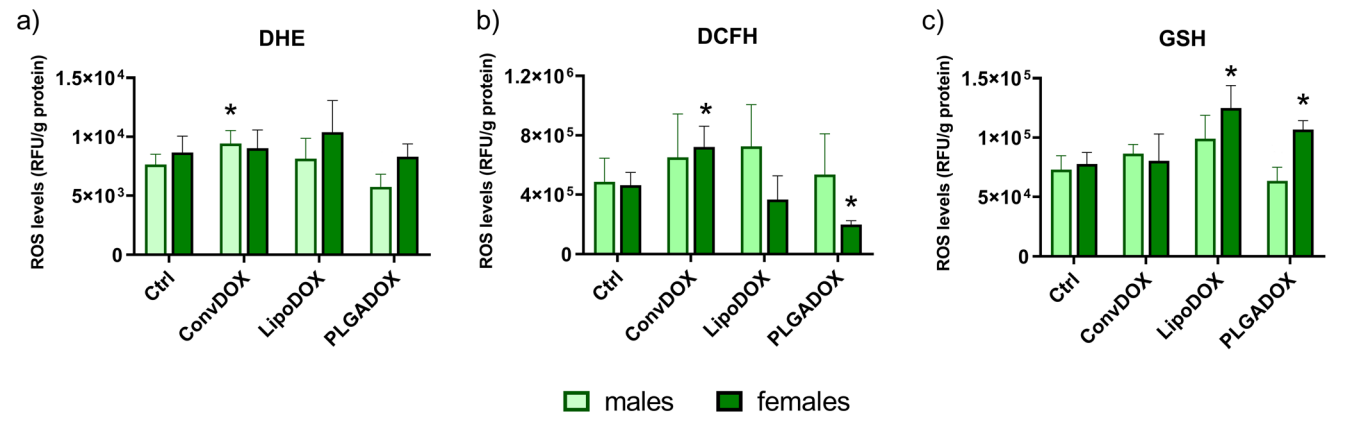

Fig. 4 Oxidative stress parameters measured in the heart tissue of control (Ctrl) male (light green columns) and female (dark green columns) rats and after administration of conventional doxorubicin (ConvDOX), a non-PEGylated liposomal formulation of doxorubicin (LipoDOX), or PLGA-based nanoformulation of doxorubicin (PLGADOX). Levels of superoxide radical (a), peroxy radical (b) and glutathione (c) are given as % of fluorescence compared to the control. Error bars: SD. *$p < 0.05$ between Ctrl and treated animals.

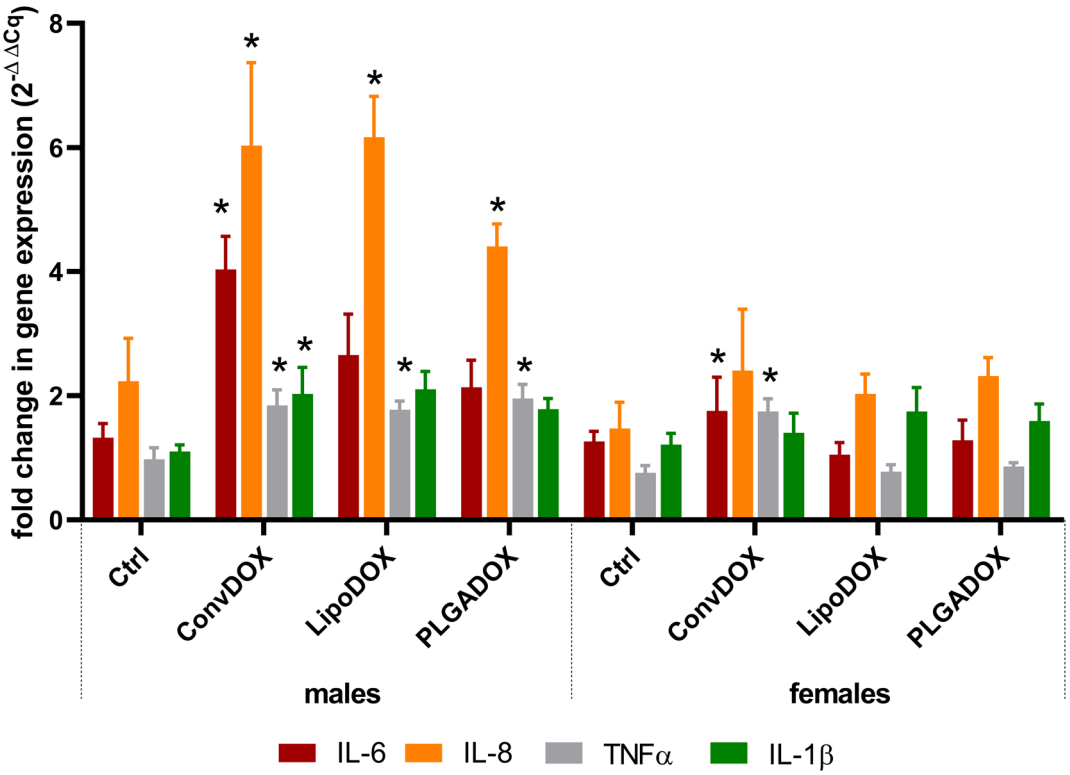

Fig. 5 Changes in gene expressions of IL-6, IL-8, TNFα and IL-1β in heart tissue of male and female rats after treatment with conventional doxorubicin (ConvDOX), non-PEGylated liposomal formulation (LipoDOX), and PLGA-based nanoformulation (PLGADOX). Shown are average values ± standard error of the mean (SEM). Significant differences between treated and control animals are denoted with an asterisk (*) at $p < 0.05$.

treated by ConvDOX formulations, while this was the case in females only for IL-6 and TNFα (Fig. 5). LipoDOX formulation significantly increased expression of IL-8, TNFα and IL-1β in males, while none of the cytokines were affected in females either by LipoDOX or by PLGADOX treatments (Fig. 5). Treatment with PLGADOX led to a similar cytokine expression profile as in LipoDOX-treated males. Again, females showed less significant inflammatory changes than males. Overall results indicate the highest inflammatory response for ConvDOX and the lowest for PLGADOX.

MSI analysis of heart tissue

In our previous study conducted on the kidneys of DOX-treated rats, we have shown that the use of MSI analysis can provide a wide variety of information for the safety profiling of drug formulations.[38] Here, we decided to focus on the metabolic and lipidomic markers involved in DOX-induced cytotoxicity and cellular response, namely spermine, Car, Cer, and LysoPC. An overview of their biological effects related to DOX toxic effects and their tentative annotations are given in Table 1.

Spermine is a natural polyamine involved in the synthesis, functioning, maintenance, and stability of nucleic acids.[75,77,80] Increased amounts are associated with cancer, inflammation, oxidative stress, and may induce autophagy,[75] while very low amounts of spermine are associated with severe cellular dysfunctions.[97] Cer are structural components of the cell membrane that participate in the formation of lipid rafts.[81] They are highly active and are involved in oxidative stress through disruptions in mitochondrial membrane[83,98] contributing to the development of cardiovascular diseases.[88] LysoPCs are minor components of the cell membrane whose expression is usually correlated to the extent of cardiac damage.[96,99]

Values of log2 average *m*/*z* intensity ratios found in the heart muscle of animals treated with different DOX formulations were divided by corresponding intensities of the untreated control animals. Results are presented in the heatmap, which shows that the greatest changes in the levels of the tentatively annotated biomarkers were observed after treatment with ConvDOX (Fig. 6 and 7).

Expression of all selected biomarkers, namely spermine, Cer, Car and LysoPC, was increased in ConvDOX case compared to the control animals. An increase in the levels of LysoPC, spermine, and Cer indicated the presence of apoptosis and inflammation processes, whereas a disturbance in mitochondrial function was indicated by an increase in Car, Cer and LysoPC levels. The only exception is the expression of medium-size carnitines in females that remained unchanged. However, the changes in LysoPC and Cer expressions were more prominent in females, suggesting more pronounced oxidative stress and apoptosis, but also, a possible cell proliferation. In contrast to ConvDOX, LipoDOX and PLGADOX had

Table 1 An overview of biomarkers related to DOX-caused cytotoxicity with their biological roles and effects

Metabolic biomarkers (MS-detectable H^+ adducts)	Tentative annotations m/z for $(M + H^+)$ adducts	Doxorubicin cytotoxicity and cellular response	Biomarker role/effect
Spermine	203.22	Topoisomerase II inhibition/ DNA intercalation Apoptosis Cell proliferation: inflammation and regeneration	Binding to nucleic acids; regulating their stability, function, and maintenance[75–77] Regulation of apoptosis[75,77–79] Increased in proliferating cells and in tissues following injury and inflammation[75,77,80]
Ceramides (Cer)	538.52 (16:0) 636.63 (23:0) 648.63 (24:1)	Binding to cell membranes Mitochondrial dysfunction and free radical formation Apoptosis Cell proliferation: inflammation and regeneration	Structural components of cell membranes; participating in the formation of lipid rafts[81–83] Increasing mitochondrial membrane permeability; disruption of electron transport; oxidative stress[83–85] Apoptotic signaling[85,86] Increased in inflammation and cellular stress[81,85,87–89]
Acyl-carnitines (Car)	428.37 (C18:0) 401.35 (C16:0) 426.36 (C18:1) 425.35 (C18:2) 258.17 (C6:1)	Mitochondrial dysfunction and free radical formation	Intermediate metabolites in fatty acid beta-oxidation in mitochondria; elevated when mitochondrial metabolism is reduced[90–92]
LysoPC	568.34 (22:6) 496.34 (16:0) 548.37 (20:2) 482.32 (15:0) 468.31 (14:0)	Mitochondrial dysfunction and free radical formation Apoptosis Cell proliferation: inflammation and regeneration	Oxidative stress[93–95] Induce apoptosis through multiple signaling pathways[93,95,96] Pro-inflammatory agents; activation of the immune system[93–95]

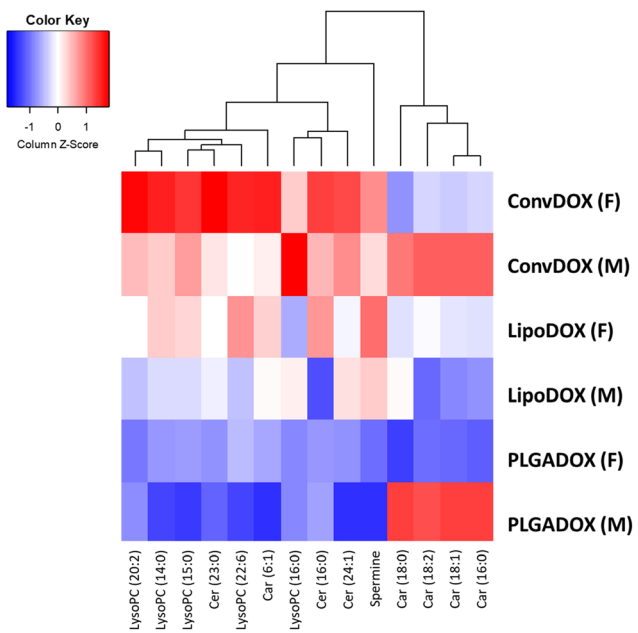

Fig. 6 Heart muscle MSI. Heat map of the log2 average m/z intensity ratios (treatment *vs.* controls): intensities of animals treated with conventional doxorubicin (ConvDOX), non-PEGylated liposomal formulation of doxorubicin (LipoDOX), or PLGA-liposomal formulation of doxorubicin (PLGADOX) were divided by corresponding intensities of the untreated controls. Each row represents two animals classified by sex and treatment.

no effect on LysoPCs expression showing the benefits of nano-formulated DOX.

IMS results are in good agreement with the described oxidative stress response. Increased levels of GSH in heart muscles of females treated by LipoDOX and PLGADOX that also produced the lowest levels of peroxy radicals were in concordance with MSI acylcarnitine' analysis: the less free radicals released from less damaged mitochondria, the more GSH and the less accumulation of acylcarnitines. The opposite is true for the PLGADOX-treated males. Interestingly, the unexpected negative trends of changes in peroxy radicals' content partially coincide with LysoPC, which is another measure of oxidative stress: the reduced levels of LysoPC, but also ceramide and spermine, in PLGADOX and, to a lesser extent, in LipoDOX case indicate reduced oxidative stress compared to ConvDOX. This may indicate the reduced basal mitochondrial function in animals treated with liposomal formulations. In agreement with this hypothesis are the existence of preapoptotic eosinophilic cells and, also relatively low interleukin responses, noted in females treated by PLGADOX and LipoDOX that may be a consequence of lower basal mitochondrial activities in immune cells that produce interleukins. The possibility of the basal mitochondrial activity's reduction not only in muscles but also in other tissues, especially in immune cells, associated with the liposomal DOX treatments, is worth further

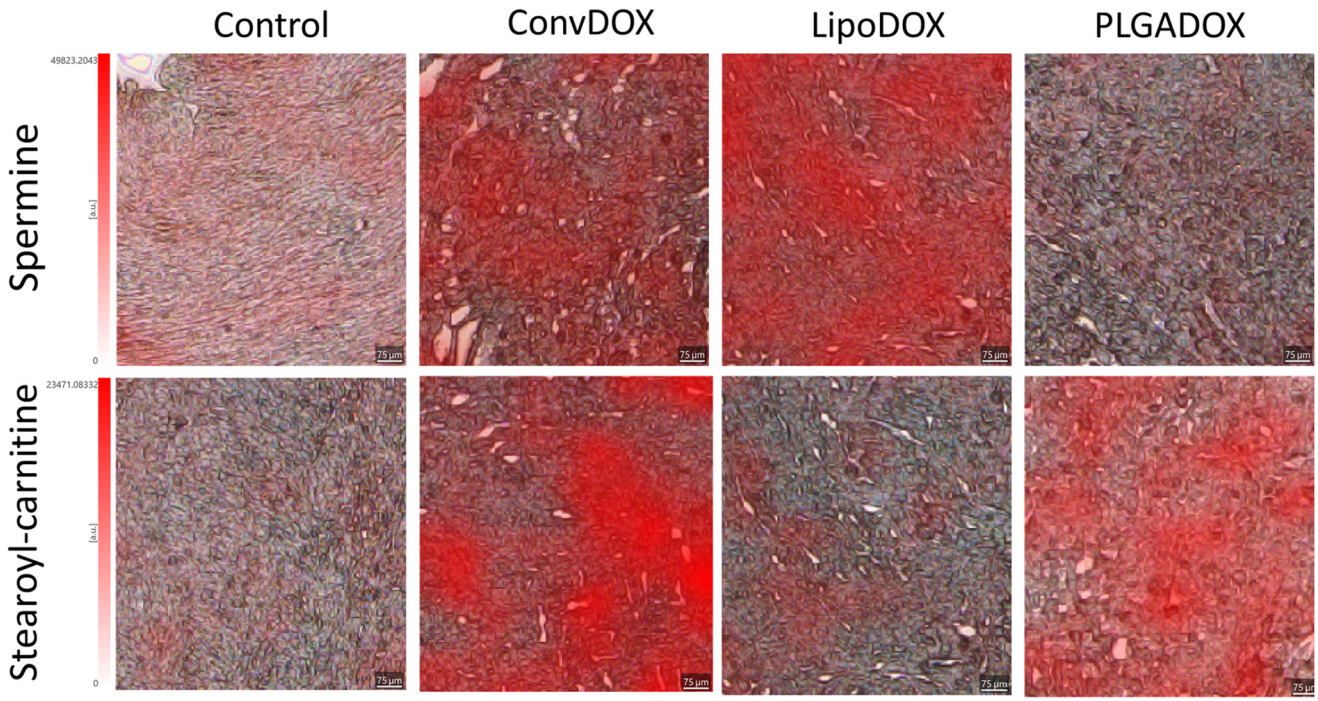

Fig. 7 Representative light microscopy native images (25×) of hearts of male rats treated with conventional (ConvDOX), liposomal (LipoDOX), or PLGA-based doxorubicin formulations (PLGADOX). Images are overlaid with the lateral distribution of tentatively annotated *m*/*z* values of 203.22 ± 0.01 Da (spermine) and 428.37 ± 0.01 Da (stearoyl-carnitine). Bars indicate 75 μm.

investigation. Amongst two nanoformulations, treatment with LipoDOX caused apoptosis and oxidative stress indicated by an increase in the levels of spermine and Cer. On the contrary, PLGADOX treatment did not affect the levels of spermine and Cer but caused an increase of medium-size Car, intermediates in the fatty acid metabolism,[90–92] implying changes in the mitochondrial metabolism in males.

The most prominent changes in lateral distributions of spermine and stearoyl-carnitine (Car 18:0), laid over the native light microscopy images of muscle preparations used for MSI are given in Fig. 7. It is visible that the changes are relatively homogenously distributed throughout the muscle tissue: the spermine and Car 18:0 contents were lower only in blood vessels. It looks like the toxic effects of analyzed DOX formulations primarily took place in the muscle tissue. This result is consistent with the fact that the signs of hemorrhage were found only in male rats, especially in the case of ConvDOX treatment: the most prominent elevations of spermine and Car C:18, primarily associated with the ConvDOX treatment of males, are visible in Fig. 7, where they even cover blood vessels. This is in agreement with results of IL-8 measurements. IL-8 is produced by macrophages and endothelial cells. ConvDOX treatment is highly associated with the IL-8 rise and increased spermine and stearoyl-carnitine content in or near the blood vessels (Fig. 7). Since the spermine and stearoyl-carnitine are associated to inflammation, apoptosis and free radical formation their localization in blood vessels that may produce IL-8 is another indicator of the possible inflammatory response's role in cardiotoxicity. The link between IL-8 production and rise of the spermine and stearoyl-carnitine tissue content, although expected, is worth of further investigation aimed at discovery of new inflammatory biomarkers of cardiotoxicity.

Conclusion

Damages caused by ConvDOX can be seen in the necrotic changes and oxidative stress response in heart tissues, increased expression of inflammation-related genes, as well as in changes in serum cardiac biomarkers. Sex-related response was found for all DOX formulations. Pathohystological analyses showed that both nanoformulations can reduce, although not fully protect from DOX-caused cardiotoxicity. All formulations caused myocardial cell injury in males indicated by an increase in TnT levels with the highest increase caused by ConvDOX treatment. The mRNA expression analyses confirmed the greatest inflammatory potential of ConvDOX formulation, which corroborated well with the markers of oxidative stress response. IMS analyses showed the greatest changes in the levels of spermine, Car, Cer and LysoPC. For DOX nanoformulations, IMS results indicated apoptosis and oxidative stress caused by LipoDOX treatment, whereas PLGADOX treatment had an effect on cell proliferation and mitochondrial damages, but only in males. Compared to PLGADOX, LipoDOX formulation caused more pronounced

alterations in the rat cardiac muscle indicating, at least, a comparable safety profile of the novel PLGADOX formulation. To conclude, novel PLGA-based DOX nanoformulations demonstrated protective action from DOX-related cardiotoxic events. As the most concerning aspect of DOX cardiotoxicity is related to the long-term effects, these results highlight the need for follow-up studies that will establish mitigation of DOX cardiotoxicity in long-term treatment by applying the protective nanoformulations.

Ethical statement

All animal procedures were performed in accordance with the EU Directive 2010/63/EU for animal experiments, with the Animal Protection Act (OG 135/06, 37/13) and the Ordinance on the protection of animals used for experimental and other scientific purposes (OG 55/13) of the Republic of Croatia, and with the Guidelines for Care and Use of Laboratory Animals of the Croatian Ministry of Agriculture, Directorate of Veterinary and Food Safety, Department of Animal Welfare. All experiments were approved by the Ethical Committee of the Croatian Ministry of Agriculture, Directorate of Veterinary and Food Safety, Department of Animal Welfare (Ethical Committee review number EP 320/2021; animal welfare approval class UP/I-322-01/21-01/08, urbr: 525-10/0543-21-4) and by the Ethical Committee of the Institute for Medical Research and Occupational Health (Ur.br: 100-21/19-24).

Conflicts of interest

There are no conflicts to declare.

Acknowledgements

We are grateful to Krunoslav Ilić, Barbara Pem and Emerik Galić for their technical help and assistance during experiments. This study was financially supported by the "Research Cooperability" Program of the Croatian Science Foundation funded by the European Union from the European Social Fund under the Operational Programme Efficient Human Resources 2014–2020 (grant HRZZ-PZS-2019-02-4323), the European Regional Development and Croatian Ministry of Science fund under the Operational Programme "Competitiveness and Cohesion 2014–2020" (grant KK.01.1.1.02.0015), and the EU H2020 project "PHOENIX – Pharmaceutical Open Innovation Test Bed for Enabling Nano-pharmaceutical Innovative Products" funded under grant agreement no. 953110.

References

1 F. Arcamone, *et al.*, Adriamycin, 14-hydroxydaimomycin, a new antitumor antibiotic from S. Peucetius var.caesius, *Biotechnol. Bioeng.*, 1969, **11**, 1101–1110.
2 G. Takemura and H. Fujiwara, Doxorubicin-Induced Cardiomyopathy., *Prog. Cardiovasc. Dis.*, 2007, **49**, 330–352.
3 Y. Octavia, *et al.*, Doxorubicin-induced cardiomyopathy: From molecular mechanisms to therapeutic strategies, *J. Mol. Cell. Cardiol.*, 2012, **52**, 1213–1225.
4 A. Shafei, *et al.*, A review on the efficacy and toxicity of different doxorubicin nanoparticles for targeted therapy in metastatic breast cancer, *Biomed. Pharmacother.*, 2017, **95**, 1209–1218.
5 K. M. Tewey, T. C. Rowe, L. Yang, B. D. Halligan and L. F. Liu, Adriamycin-Induced DNA Damage Mediated by Mammalian DNA Topoisomerase II, *Science*, 1984, **226**(4673), 466–468.
6 M. Tokarska-Schlattner, M. Zaugg, C. Zuppinger, T. Wallimann and U. Schlattner, New insights into doxorubicin-induced cardiotoxicity: The critical role of cellular energetics, *J. Mol. Cell. Cardiol.*, 2006, **41**, 389–405.
7 J. Pawłowska, J. Tarasiuk, C. R. Wolf, M. J. I. Paine and E. Borowski, Differential Ability of Cytostatics From Anthraquinone Group to Generate Free Radicals in Three Enzymatic Systems: NADH Dehydrogenase, NADPH Cytochrome P450 Reductase, and Xanthine Oxidase, *Oncol. Res.*, 2003, **13**, 245–252.
8 S. Sritharan and N. Sivalingam, A comprehensive review on time-tested anticancer drug doxorubicin, *Life Sci.*, 2021, **278**, 119527.
9 S. Geiger, V. Lange, P. Suhl, V. Heinemann and H.-J. Stemmler, Anticancer therapy induced cardiotoxicity: review of the literature, *Anticancer. Drugs*, 2010, **21**, 578–590.
10 J. Salazar-Mendiguchía, *et al.*, Anthracycline-mediated cardiomyopathy: Basic molecular knowledge for the cardiologist, *Arch. Cardiol.*, 2014, **84**, 218–223.
11 J. Liu, *et al.*, Quality of Life Analyses in a Clinical Trial of DPPE (tesmilifene) Plus Doxorubicin Versus Doxorubicin in Patients with Advanced or Metastatic Breast Cancer: NCIC CTG Trial MA.19, *Breast Cancer Res. Treat.*, 2006, **100**, 263–271.
12 T. M. Zagar, D. M. Cardinale and L. B. Marks, Breast cancer therapy-associated cardiovascular disease, *Nat. Rev. Clin. Oncol.*, 2016, **13**, 172–184.
13 P. K. Singal and N. Iliskovic, Doxorubicin-Induced Cardiomyopathy., *N. Engl. J. Med.*, 1998, **339**, 900–905.
14 D. D. Von Hoff, Risk, Factors for Doxorubicin-lnduced Congestive Heart Failure, *Ann. Intern. Med.*, 1979, **91**, 710.
15 P. S. Rawat, A. Jaiswal, A. Khurana, J. S. Bhatti and U. Navik, Doxorubicin-induced cardiotoxicity: An update on the molecular mechanism and novel therapeutic strategies for effective management, *Biomed. Pharmacother.*, 2021, **139**, 111708.
16 S.-I. Kanno and A. Hara, The mRNA expression of Il6 and Pdcd1 are predictive and protective factors for doxorubicin-induced cardiotoxicity, *Mol. Med. Rep.*, 2020, **23**, 113.
17 A. Avagimyan, L. Kakturskiy, K. Heshmat-Ghahdarijani, N. Pogosova and N. Sarrafzadegan, Anthracycline Associated Disturbances of Cardiovascular Homeostasis, *Curr. Probl. Cardiol.*, 2022, **47**, 100909.

18 L. A. Smith, *et al.*, Cardiotoxicity of anthracycline agents for the treatment of cancer: Systematic review and meta-analysis of randomised controlled trials, *BMC Cancer*, 2010, **10**, 337.
19 M. R. Bristow, J. W. Mason, M. E. Billingham and J. R. Daniels, Dose-effect and structure-function relationships in doxorubicin cardiomyopathy, *Am. Heart J.*, 1981, **102**, 709–718.
20 E. C. van Dalen, H. N. Caron, H. O. Dickinson and L. C. Kremer, Cardioprotective interventions for cancer patients receiving anthracyclines, in *Cochrane Database of Systematic Reviews*, ed. E. C. van Dalen, John Wiley & Sons, Ltd, 2008, DOI: 10.1002/14651858.CD003917.pub3.
21 S. S. Nunes, *et al.*, PEGylated versus Non-PEGylated pH-Sensitive Liposomes: New Insights from a Comparative Antitumor Activity Study, *Pharmaceutics*, 2022, **14**, 272.
22 S. S. Nunes, *et al.*, Influence of PEG coating on the biodistribution and tumor accumulation of pH-sensitive liposomes, *Drug Delivery Transl. Res.*, 2019, **9**, 123–130.
23 W. Brand, *et al.*, Nanomedicinal products: a survey on specific toxicity and side effects, *Int. J. Nanomed.*, 2017, **12**, 6107–6129.
24 C. E. Swenson, W. R. Perkins, P. Roberts and A. S. Janoff, Liposome technology and the development of MyocetTM (liposomal doxorubicin citrate), *Breast*, 2001, **10**, 1–7.
25 R. C. F. Leonard, S. Williams, A. Tulpule, A. M. Levine and S. Oliveros, Improving the therapeutic index of anthracycline chemotherapy: Focus on liposomal doxorubicin (Myocet™), *Breast*, 2009, **18**, 218–224.
26 A. Gagliardi, *et al.*, Cardiotoxicity and Treatment Efficacy of Not Pegilated Liposomal Doxorubicin in Haematological Malignancies: Our Experience, *Blood*, 2007, **110**, 4836–4836.
27 M. Marty, Liposomal doxorubicin (Myocet™) and conventional anthracyclines: a comparison, *Breast*, 2001, **10**, 28–33.
28 G. Batist, *et al.*, Reduced Cardiotoxicity and Preserved Antitumor Efficacy of Liposome-Encapsulated Doxorubicin and Cyclophosphamide Compared With Conventional Doxorubicin and Cyclophosphamide in a Randomized, Multicenter Trial of Metastatic Breast Cancer, *J. Clin. Oncol.*, 2001, **19**, 1444–1454.
29 X.-R. Li, X.-H. Cheng, G.-N. Zhang, X.-X. Wang and J.-M. Huang, Cardiac safety analysis of first-line chemotherapy drug pegylated liposomal doxorubicin in ovarian cancer, *J. Ovarian Res.*, 2022, **15**, 96.
30 M. Xing, F. Yan, S. Yu and P. Shen, Efficacy and Cardiotoxicity of Liposomal Doxorubicin-Based Chemotherapy in Advanced Breast Cancer: A Meta-Analysis of Ten Randomized Controlled Trials, *PLoS One*, 2015, **10**, e0133569.
31 M. Mohamed, *et al.*, PEGylated liposomes: immunological responses, *Sci. Technol. Adv. Mater.*, 2019, **20**, 710–724.
32 D. S. Alberts, *et al.*, Efficacy and safety of liposomal anthracyclines in Phase I/II clinical trials, *Semin. Oncol.*, 2004, **31**, 53–90.
33 C. V. Rocha, V. Gonçalves, M. C. da Silva, M. Bañobre-López and J. Gallo, PLGA-Based Composites for Various Biomedical Applications, *Int. J. Mol. Sci.*, 2022, **23**, 2034.
34 T. Sonam Dongsar, T. Tsering Dongsar, N. Molugulu, S. Annadurai, S. Wahab, N. Gupta and P. Kesharwani, Targeted therapy of breast tumor by PLGA-based nanostructures: The versatile function in doxorubicin delivery, *Environ. Res.*, 2023, **233**, 116455.
35 E. Pereverzeva, I. Treschalin, M. Treschalin, D. Arantseva, Y. Ermolenko, N. Kumskova, O. Maksimenko, V. Balabanyan, J. Kreuter and S. Gelperina, Toxicological study of doxorubicin-loaded PLGA nanoparticles for the treatment of glioblastoma, *Int. J. Pharm.*, 2019, **554**, 161–178.
36 M. Alvi, A. Yaqoob, K. Rehman, *et al.*, PLGA-based nanoparticles for the treatment of cancer: current strategies and perspectives, *AAPS Open*, 2022, **8**, 12.
37 E. L. J. Moya, S. M. Lombardo, E. Vandenhaute, M. Schneider, C. Mysiorek, A. E. Türeli, T. Kanda, F. Shimizu, Y. Sano, N. Maubon, F. Gosselet, N. Günday-Türeli and M.-P. Dehouck, Interaction of surfactant coated PLGA nanoparticles with in vitro human brain-like endothelial cells, *Int. J. Pharm.*, 2022, **621**, 121780.
38 Ž Debeljak, *et al.*, Imaging mass spectrometry differentiates the effects of doxorubicin formulations on non-targeted tissues, *Analyst*, 2022, **147**, 3201–3208.
39 X. Luo, B. Reichetzer, J. Trines, L. N. Benson and D. C. Lehotay, L-carnitine attenuates doxorubicin-induced lipid peroxidation in rats, *Free Radical Biol. Med.*, 1999, **26**, 1158–1165.
40 E. Pereverzeva, *et al.*, Intravenous tolerance of a nanoparticle-based formulation of doxorubicin in healthy rats, *Toxicol. Lett.*, 2008, **178**, 9–19.
41 J. Robert, Preclinical assessment of anthracycline cardiotoxicity in laboratory animals: Predictiveness and pitfalls, *Cell Biol. Toxicol.*, 2007, **23**, 27–37.
42 K. Golla, B. Cherukuvada, F. Ahmed and A. K. Kondapi, Efficacy, Safety and Anticancer Activity of Protein Nanoparticle-Based Delivery of Doxorubicin through Intravenous Administration in Rats, *PLoS One*, 2012, **7**, e51960.
43 M. Ćurlin, *et al.*, Sex affects the response of Wistar rats to polyvinyl pyrrolidone (PVP)-coated silver nanoparticles in an oral 28 days repeated dose toxicity study, *Part. Fibre Toxicol.*, 2021, **18**, 38.
44 J. Hellemans, G. Mortier, A. De Paepe, F. Speleman and J. Vandesompele, qBase relative quantification framework and software for management and automated analysis of real-time quantitative PCR data, *Genome Biol.*, 2007, **8**, R19.
45 R Core Team R: A Language and Environment for Statistical Computing. R Foundation for Statistical Computing, Vienna, Austria, 2023, <https://www.R-project.org/>.
46 P. Xia, *et al.*, Doxorubicin induces cardiomyocyte apoptosis and atrophy through cyclin-dependent kinase 2-mediated activation of forkhead box O1, *J. Biol. Chem.*, 2020, **295**, 4265–4276.

47 Y. M. Jang, *et al.*, Doxorubicin treatment in vivo activates caspase-12 mediated cardiac apoptosis in both male and female rats, *FEBS Lett.*, 2004, **577**, 483–490.
48 L. Cove-Smith, *et al.*, An Integrated Characterization of Serological, Pathological, and Functional Events in Doxorubicin-Induced Cardiotoxicity, *Toxicol. Sci.*, 2014, **140**, 3–15.
49 J. P. Stice, J. S. Lee, A. S. Pechenino and A. A. Knowlton, Estrogen, aging and the cardiovascular system, *Future Cardiol.*, 2009, **5**, 93–103.
50 M. A. Choudhry and I. H. Chaudry, 17β-Estradiol: a novel hormone for improving immune and cardiovascular responses following trauma-hemorrhage, *J. Leukocyte Biol.*, 2008, **83**, 518–522.
51 L.-L. Tan and A. R. Lyon, Role of Biomarkers in Prediction of Cardiotoxicity During Cancer Treatment, *Curr. Treat. Options Cardiovasc. Med.*, 2018, **20**, 55.
52 J.-P. Bertinchant, *et al.*, Release kinetics of serum cardiac troponin i in ischemic myocardial injury, *Clin. Biochem.*, , 1996, **29**, 587–594.
53 L. Michel, *et al.*, Troponins and brain natriuretic peptides for the prediction of cardiotoxicity in cancer patients: a meta–analysis, *Eur. J. Heart Failure*, 2020, **22**, 350–361.
54 I. Germanakis, *et al.*, Correlation of plasma N-terminal pro-brain natriuretic peptide levels with left ventricle mass in children treated with anthracyclines, *Int. J. Cardiol.*, 2006, **108**, 212–215.
55 F. Dodos, T. Halbsguth, E. Erdmann and U. C. Hoppe, Usefulness of myocardial performance index and biochemical markers for early detection of anthracycline-induced cardiotoxicity in adults, *Clin. Res. Cardiol.*, 2008, **97**, 318–326.
56 E. H. Herman, *et al.*, Use of cardiac troponin T levels as an indicator of doxorubicin-induced cardiotoxicity, *Cancer Res.*, 1998, **58**, 195–197.
57 E. Murphy, *et al.*, Mechanism of Cardioprotection: What Can We Learn from Females?, *Pediatr. Cardiol.*, 2011, **32**, 354–359.
58 Y. Zheng, *et al.*, Low NT-proBNP levels: An early sign for the diagnosis of ischemic heart failure, *Int. J. Cardiol.*, 2017, **228**, 666–671.
59 B. Ky, *et al.*, Early Increases in Multiple Biomarkers Predict Subsequent Cardiotoxicity in Patients With Breast Cancer Treated With Doxorubicin, Taxanes, and Trastuzumab, *J. Am. Coll. Cardiol.*, 2014, **63**, 809–816.
60 H. Sawaya, *et al.*, Assessment of Echocardiography and Biomarkers for the Extended Prediction of Cardiotoxicity in Patients Treated With Anthracyclines, Taxanes, and Trastuzumab, *Circ. Cardiovasc. Imaging*, 2012, **5**, 596–603.
61 M. T. Sandri, *et al.*, N-Terminal Pro-B-Type Natriuretic Peptide after High-Dose Chemotherapy: A Marker Predictive of Cardiac Dysfunction?, *Clin. Chem.*, 2005, **51**, 1405–1410.
62 A. Pieniążek, J. Czepas, J. Piasecka-Zelga, K. Gwoździński and A. Koceva-Chyła, Oxidative stress induced in rat liver by anticancer drugs doxorubicin, paclitaxel and docetaxel, *Adv. Med. Sci.*, 2013, **58**, 104–111.
63 M. F. R. Zare, *et al.*, Apigenin attenuates doxorubicin induced cardiotoxicity via reducing oxidative stress and apoptosis in male rats, *Life Sci.*, 2019, **232**, 116623.
64 A. M. Rahman, S. W. Yusuf and M. S. Ewer, Anthracycline-induced cardiotoxicity and the cardiac-sparing effect of liposomal formulation, *Int. J. Nanomed.*, 2007, **2**, 567–583.
65 C. Carvalho, *et al.*, Doxorubicin: The Good, the Bad and the Ugly Effect, *Curr. Med. Chem.*, 2009, **16**, 3267–3285.
66 M. Lamberti, *et al.*, Animal Models in Studies of Cardiotoxicity Side Effects from Antiblastic Drugs in Patients and Occupational Exposed Workers, *BioMed Res. Int.*, 2014, **2014**, 1–8.
67 Y. Yoda, M. Nakazawa, T. Abe and Z. Kawakami, Prevention of doxorubicin myocardial toxicity in mice by reduced glutathione, *Cancer Res.*, 1986, **46**, 2551–2556.
68 F. Villani, *et al.*, Effect of Glutathione and N-Acetylcysteine on in Vitro and in Vivo Cardiac Toxicity of Doxorubicin, *Free Radical Res. Commun.*, 1990, **11**, 145–151.
69 V. P. Bajic, *et al.*, Glutathione "Redox Homeostasis" and Its Relation to Cardiovascular Disease, *Oxid. Med. Cell. Longevity*, 2019, **2019**, 1–14.
70 L. Dong, *et al.*, A pH/Enzyme-responsive tumor-specific delivery system for doxorubicin, *Biomaterials*, 2010, **31**, 6309–6316.
71 A. Kaczmarek, B. M. Brinkman, L. Heyndrickx, P. Vandenabeele and D. V. Krysko, Severity of doxorubicin-induced small intestinal mucositis is regulated by the TLR-2 and TLR-9 pathways, *J. Pathol.*, 2012, **226**, 598–608.
72 A. D. Leal, *et al.*, Fosaprepitant-induced phlebitis: a focus on patients receiving doxorubicin/cyclophosphamide therapy, *Support. Care Cancer*, 2014, **22**, 1313–1317.
73 B. W. Van Tassell, S. Toldo, E. Mezzaroma and A. Abbate, Targeting Interleukin-1 in Heart Disease, *Circulation*, 2013, **128**, 1910–1923.
74 A. Reis-Mendes, *et al.*, Role of Inflammation and Redox Status on Doxorubicin-Induced Cardiotoxicity in Infant and Adult CD-1 Male Mice, *Biomolecules*, 2021, **11**, 1725.
75 R. Amendola, *et al.*, Spermine Metabolism and Anticancer Therapy, *Curr. Cancer Drug Targets*, 2009, **9**, 118–130.
76 N. A. Sagar, S. Tarafdar, S. Agarwal, A. Tarafdar and S. Sharma, Polyamines: Functions, Metabolism, and Role in Human Disease Management, *Med. Sci.*, 2021, **9**, 44.
77 C. Wang, *et al.*, Ultra-Performance Liquid Chromatography-Q-Exactive Orbitrap-Mass Spectrometry Analysis for Metabolic Communication between Heart and Kidney in Adriamycin-Induced Nephropathy Rats, *Kidney Blood Pressure Res.*, 2022, **47**, 31–42.
78 M. Zhang, H. Wang and K. J. Tracey, Regulation of macrophage activation and inflammation by spermine: A new chapter in an old story, *Crit. Care Med.*, 2000, **28**, N60–N66.
79 R. A. Casero and L. J. Marton, Targeting polyamine metabolism and function in cancer and other hyperproliferative diseases, *Nat. Rev. Drug Discovery*, 2007, **6**, 373–390.

80 Y. Y. Lenis, M. A. Elmetwally, J. G. Maldonado-Estrada and F. W. Bazer, Physiological importance of polyamines, *Zygote*, 2017, **25**, 244–255.
81 W. J. Blitterswijk, A. H. van Luit, R. J. van der Veldman, M. Verheij and J. Borst, Ceramide: second messenger or modulator of membrane structure and dynamics?, *Biochem. J.*, 2003, **369**, 199–211.
82 A. Morales, H. Lee, F. M. Goñi, R. Kolesnick and J. C. Fernandez-Checa, Sphingolipids and cell death, *Apoptosis*, 2007, **12**, 923–939.
83 A. Millner and G. E. Atilla-Gokcumen, Solving the enigma: Mass spectrometry and small molecule probes to study sphingolipid function, *Curr. Opin. Chem. Biol.*, 2021, **65**, 49–56.
84 S. M. Turpin-Nolan and J. C. Brüning, The role of ceramides in metabolic disorders: when size and localization matters, *Nat. Rev. Endocrinol.*, 2020, **16**, 224–233.
85 W. Yun, L. Qian, R. Yuan and H. Xu, Periplocymarin Alleviates Doxorubicin-Induced Heart Failure and Excessive Accumulation of Ceramides, *Front. Cardiovasc. Med.*, 2021, **8**, 732554.
86 B. T. Bikman and S. A. Summers, Ceramides as modulators of cellular and whole-body metabolism, *J. Clin. Invest.*, 2011, **121**, 4222–4230.
87 J. Woodcock, Sphingosine and ceramide signalling in apoptosis, *IUBMB Life*, 2006, **58**, 462–466.
88 R. H. Choi, S. M. Tatum, J. D. Symons, S. A. Summers and W. L. Holland, Ceramides and other sphingolipids as drivers of cardiovascular disease, *Nat. Rev. Cardiol.*, 2021, **18**, 701–711.
89 S. A. F. Morad and M. C. Cabot, Ceramide-orchestrated signalling in cancer cells, *Nat. Rev. Cancer*, 2013, **13**, 51–65.
90 M. R. McCann, M. V. George De la Rosa, G. R. Rosania and K. A. Stringer, L-Carnitine and Acylcarnitines: Mitochondrial Biomarkers for Precision Medicine, *Metabolites*, 2021, **11**, 51.
91 D. K. Perry and Y. A. Hannun, The role of ceramide in cell signaling, *Biochim. Biophys. Acta, Mol. Cell Biol. Lipids*, 1998, **1436**, 233–243.
92 C. S. McCoin, T. A. Knotts and S. H. Adams, Acylcarnitines—old actors auditioning for new roles in metabolic physiology, *Nat. Rev. Endocrinol.*, 2015, **11**, 617–625.
93 Q. Zhou, *et al.*, The compatibility effects of sini decoction against doxorubicin-induced heart failure in rats revealed by mass spectrometry-based serum metabolite profiling and computational analysis, *J. Ethnopharmacol.*, 2020, **252**, 112618.
94 Y. Li, *et al.*, Screening, Verification, and Optimization of Biomarkers for Early Prediction of Cardiotoxicity Based on Metabolomics, *J. Proteome Res.*, 2015, **14**, 2437–2445.
95 P. Liu, *et al.*, The mechanisms of lysophosphatidylcholine in the development of diseases, *Life Sci.*, 2020, **247**, 117443.
96 S.-H. Law, *et al.*, An Updated Review of Lysophosphatidylcholine Metabolism in Human Diseases, *Int. J. Mol. Sci.*, 2019, **20**, 1149.
97 S. Mandal, A. Mandal, H. E. Johansson, A. V. Orjalo and M. H. Park, Depletion of cellular polyamines, spermidine and spermine, causes a total arrest in translation and growth in mammalian cells, *Proc. Natl. Acad. Sci. U. S. A.*, 2013, **110**, 2169–2174.
98 L. J. Siskind, Mitochondrial Ceramide and the Induction of Apoptosis, *J. Bioenerg. Biomembr.*, 2005, **37**, 143–153.
99 C. K. Ward-Caviness, *et al.*, Improvement of myocardial infarction risk prediction via inflammation-associated metabolite biomarkers, *Heart*, 2017, **103**, 1278–1285.